

# Signal Extraction and Length Sensing for LIGO II RSE

James Mason and Phil Willems\*

\* *California Institute of Technology, Pasadena, California 91125*

**Abstract.** In anticipation of an upgrade of the LIGO detector to an advanced configuration in 2004, a tabletop prototype of resonant sideband extraction is being designed and constructed at Caltech. We present here two frontally modulated length sensing and control schemes, one in which the signal extraction/recycling mirror is a simple mirror, and one in which it is a Fabry-Perot cavity. Issues regarding the controllability, RF sideband transmission, shot noise, and noise couplings are discussed.

Advanced detectors for the LIGO interferometer are planned which use a configuration in which the position of a mirror at the output is used to tune the frequency response, such as resonant sideband extraction (RSE) [1] or dual recycling [2]. RSE can also allow for the storage time of carrier light in the Fabry-Perot arms to be increased, hence the power recycling in the interferometer can be made smaller, reducing thermal lensing in transmissive optics such as the beamsplitter or input test masses without reducing the bandwidth of the detector to gravitational waves.

The sensitivity of RSE is well understood [3], but issues of control, lock acquisition and signal extraction are still open, and are the subject of our research. We are considering schemes that, like LIGO I, employ frontal modulation, and which use a set of fixed sidebands on the optical carrier so as to guarantee transmission of all sidebands through an input mode cleaner before entering the interferometer, regardless of the tuning of the output mirror.

In LIGO, the signal extraction and control are sensitive to the sideband transmission through the interferometer. The RF sideband transmission to the dark port is well approximated by a three-mirror coupled cavity consisting of the input power recycling mirror, the compound mirror formed by the Michelson interferometer (i.e., the beamsplitter and arm mirrors), and the output signal extraction mirror. In the broadband mode of RSE, where the signal extraction cavity (SEC) is resonant for the optical carrier, both RF sidebands are resonant in this three-mirror cavity and are efficiently transmitted to the output. However, in detuned RSE, when the signal extraction cavity is not resonant for the optical carrier, the

CP523, *Gravitational Waves: Third Edoardo Amaldi Conference*, edited by S. Meshkov  
© 2000 American Institute of Physics 1-56396-944-0/00/\$17.00

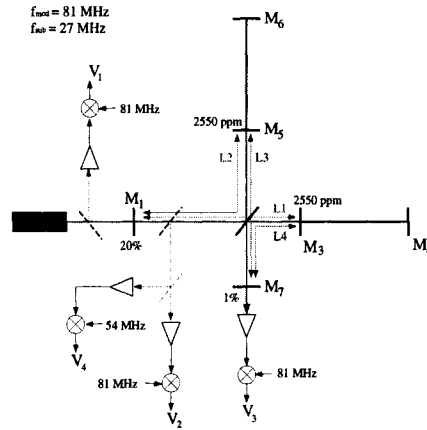


FIGURE 1. Optical configuration for RSE with a single output mirror.

two RF sidebands cannot both be transmitted with high efficiency, and they will resonate unequally in the interferometer.

We have identified two schemes for implementing RSE which address the problem of RF sideband transmission while detuned. The first, or single-sideband, scheme (SSB) accepts the loss of one RF sideband and detunes by making a macroscopic change in the signal extraction mirror position, thus allowing one RF sideband to resonate in the SEC. Once this macroscopic position is chosen there is a limited range of additional detuning that is gotten by microscopic length changes to the SEC. Compared to having both RF sidebands at the dark port, this scheme gives one-half the signal but also  $\sqrt{3}$  less shot noise, so the sensitivity is degraded only slightly. However, the unequal power buildup in the two RF sidebands introduces cross couplings into many of the degrees of freedom of the interferometer as seen by the length sensing pickoffs.

The second scheme is to replace the signal extraction mirror with an output coupling cavity (OCC) that is optimally coupled for the RF sidebands and antiresonant for the carrier. This makes the OCC ‘invisible’ to the RF sidebands so that they resonate in the interferometer exactly as in the well-understood power-recycled case. The RF sidebands transmit with high efficiency for all detunings, which can be obtained through only microscopic changes in the SEC length, and the standard shot-noise-limited sensitivity is restored. All this comes at the price of additional complexity at having to control another suspended mirror.

The SSB scheme (displayed in Figure 1) requires an independent local oscillator to measure the RF sideband phase variation in the SEC. We add a frequency-shifted subcarrier at one-third the RF modulation frequency  $f_{\text{mod}}$ . This frequency can pass through an input mode cleaner and resonate in a power recycling cavity of suitable length. We then use the beatnote at  $f_{\text{mod}} - f_{\text{mod}}/3$  at the PRC pickoff (labelled

**TABLE 1.** Matrix of discriminants for the single-sideband RSE scheme. Initial values are for no detuning (broadband case), and values in parentheses are for high detuning (narrowband case). Boldface values represent signals used for length sensing.

PD	$\Phi_+$	$\Phi_-$	$I_{81\text{MHz}}$ $\phi_+$	$\phi_-$	$\phi_s$
1	130(-1400)	0(0)	<b>-0.26(.50)</b>	0(-.53)	-3.7(-1.6)
2	<b>-1.6e4(-2.3e4)</b>	0(-1.7e-2)	1.1(-4.3)	0(-26)	-180(-80)
3	0(0)	<b>73(43)</b>	0(0)	.046(.027)	0(0)
			$Q_{81\text{MHz}}$		
1	0(-730)	-1.1e-3(0)	0(.32)	-1.6(-1.2)	0(.27)
2	0(-3600)	-5.1e-2(-3.9e-2)	0(-4.5)	<b>-81(-61)</b>	0(13)
3	0(0)	0(-14)	0(0)	0(-9.0e-3)	0(0)
			$I_{54\text{MHz}}$		
1	-1.2e-3(-1.2e-3)	0(0)	-.11(-.11)	0(0)	-2.0(-2.0)
2	-1.3e-2(-1.3e-2)	0(0)	.88(.88)	-7.4e-3(-7.3e-3)	<b>-19(-19)</b>
3	0(0)	0(0)	0(0)	5.3e-3(5.3e-3)	0(0)

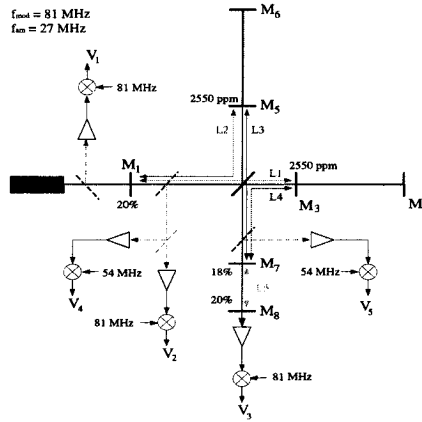


**FIGURE 2.** Optical configuration for RSE with an output-coupling cavity.

$V_4$ ) to control the SEC length. The control signal for the SEC is independent of detuning; however, those for the other degrees of freedom of the interferometer are not. As mentioned earlier, cross-couplings occur and are strong when the SEC is slightly detuned. For highly detuned RSE, the cross couplings are weaker, but the signal gains tend to change by as much as an order of magnitude for reasonable ranges of detuning. Sample control matrices for the broadband and detuned cases are shown in Table 1. Note that the cavity signals are taken from the demodulation of the optical signals at the pickoffs both in phase with (I) and in quadrature to (Q) the local oscillator.

The OCC scheme uses AM sidebands at  $f_{\text{mod}}/3$ , as well as another pickoff signal

**TABLE 2.** Matrix of discriminants for the output-coupling cavity scheme.

PD	$\Phi_+$	$\Phi_-$	$I_{81\text{MHz}}$ $\phi_+$	$\phi_-$	$\phi_s$	$\phi_{\text{occ}}$
1	73(72)	0(0)	<b>.15(.15)</b>	0(0)	0(0)	-.22(-.22)
2	<b>1.7e4(1.7e4)</b>	0(0)	-.71(-.71)	0(0)	-2.5e-2(-2.5e-2)	-11(-11)
3	0(0)	9.2(9.2)	0(0)	5.8e-3(5.8e-3)	0(0)	0(0)
4	0(0)	0(0)	0(0)	0(0)	0(0)	0(0)
			$Q_{81\text{MHz}}$			
1	0(0)	0(0)	0(0)	9.7e-2(9.7e-2)	0(0)	0(0)
2	0(0)	3e-3(3e-3)	0(0)	<b>4.7(4.7)</b>	0(0)	0(0)
3	0(0)	0(0)	0(0)	0(0)	0(0)	0(0)
4	0(0)	<b>-77(-77)</b>	0(0)	-4.9e-2(-4.9e-2)	0(0)	0(0)
			$I_{54\text{MHz}}$			
1	0(0)	0(0)	-.18(-.23)	0(.12)	0(0)	.19(.17)
2	0(0)	0(0)	.30(.34)	-1.3(-.87)	<b>-1.5(-2.1)</b>	-.21(-.30)
3	0(0)	0(0)	0(.32)	0(.86)	0(.18)	<b>-.65(-.62)</b>
4	0(0)	0(0)	0(0)	6.3e-2(6.6e-2)	0(0)	0(0)

(shown as  $V_5$  in Figure 2). The beat note at this pickoff provides signal for length control of the OCC, while the pickoff at the PRC provides signal for the SEC length. As seen in Table 2, the control matrix for this scheme is more diagonal for both the broadband and the detuned case. The degrees of freedom for the power-recycled Michelson portion of the interferometer are barely dependent upon detuning. The degrees of freedom for the signal extraction cavity and output coupling cavity are also only weakly dependent on detuning for many designs. The layout for the OCC scheme is shown in Figure 2.

We have begun experiments to test these LSC schemes using a fixed-mirror tabletop interferometer before trying them on a more representative and more complicated interferometer using suspended mirrors. These experiments will help to evaluate the advantages and disadvantages of the two schemes and to investigate the process of interferometer lock acquisition. Our power recycled arm cavity has been tested and characterized (our arm finesse is  $\sim 1000$ ), and we have characterized our power recycled Michelson and signal recycled Michelson interferometers without the arm cavities and found them to be in excellent agreement with our models. We have also locked the dual-recycled Michelson interferometer, and are beginning to introduce the  $f_{\text{mod}}/3$  subcarrier into the interferometer and test detuned RSE schemes.

## REFERENCES

1. Jun Mizuno, Ph.D. thesis, Max-Planck-Institut für Quantenoptik, 1995.
2. Strain, K. A. and B. J. Meers, *Physical Review Letters* **66**, 1391 (1991).
3. Heinzl, G. *et al.*, *Physics Letters A* **217**, 305 (1996).